Polyhedron 88 (2015) 164–169

Contents lists available at ScienceDirect

Polyhedron

journal homepage: www.elsevier.com/locate/poly

Hydrothermal synthesis and characterization of $\{[Ni_2(NA)_4(\mu\text{-}H_2O)]\cdot 2H_2O\}_n$ (HNA = nicotinic acid) and its heterogeneous catalytic effect

Burak Ay [a,*], Gözde Yağ [a], Emel Yildiz [a], Arnold L. Rheingold [b]

[a] *Department of Chemistry, Arts and Science Faculty, Cukurova University, Balcali 01330, Adana, Turkey*
[b] *Department of Chemistry and Biochemistry, University of California at San Diego, La Jolla, CA 92093, USA*

ARTICLE INFO

Article history:
Received 13 October 2014
Accepted 15 December 2014
Available online 10 January 2015

Keywords:
Hydrothermal reaction
2,3-Pyridinedicarboxylic acid
Heterogeneous catalysis
Thymoquinone
Ni(II) coordination polymer

ABSTRACT

A carboxylate-bridged metal–organic coordination polymer $\{[Ni_2(NA)_4(\mu\text{-}H_2O)]\cdot 2H_2O\}_n$ (**1**, HNA = nicotinic acid) has been synthesized under hydrothermal conditions and characterized by FT-IR, TG/DTA, micro analysis and single-crystal X-ray diffraction. **1** has an interesting 3D network structure and adjacent networks are further connected together via strong π–π packing interactions. The thermal behavior and catalytic performance of **1** were investigated and its selectivity was measured as 100% for the oxidation of thymol (T) to thymoquinone (TQ).

1. Introduction

Metal–organic frameworks (MOFs) including multifunctional carboxylic acid ligands have attracted considerable attention because of their interesting structural motifs and potential applications in different areas [1,2]. Additionally, MOFs containing nickel are widely used in several catalytic reactions, such as oxidation, hydrogen production, isomerization and dehydrogenation reactions [3]. Carboxylic acid ligands bearing oxygen and nitrogen donor atoms are the most widely used compounds for the synthesis of MOFs [4–6]. All kinds of rigid pyridinedicarboxylic (pydc) acids (2,3-, 2,4-, 2,5-, 2,6-, 3,4-, 3,5-) are good choices for constructing MOFs due to the coexistence of reliable pyridyl groups as well as carboxylate moieties with rich coordination modes [7–13]. With these ligands, a large number of beautiful networks of ingenious design have been constructed [14–20]. However, compared with other pyridinedicarboxylic acids, the use of the 2,3-pydc^{2-} ligand in heterometal–organic frameworks chemistry has been very limited [21,22]. The first reason for this is that this ligand prefers decarboxylation of the 2-position carboxylate group which transforms it to nicotinic acid under the hydrothermal conditions. Secondly, it often behaves like picolinic acid (Scheme 1), acting as a chelating bidentate ligand through the nitrogen atom and one oxygen atom of the 2-position carboxylate group, and the 3-position carboxyl group remains idle [23–25].

The hydrothermal method has been a promising technique in preparing novel coordination polymers [26]. In particular, pyridinedicarboxylic acids have been proven to be interesting and versatile ligands and may exhibit various coordination modes to build different structures with higher dimensions [27,28]. Factors such as solvent, pH and reaction temperature appear to control the dimensionality, though the different coordination compounds of the metal ions also play an important role in determining the crystal structures of the corresponding metal–organic polymers [29].

One of the potential applications of MOFs including carboxylic acid ligands is the oxidation of organic compounds. Monoterpenes are extensively used in industrial and medical areas as a starting agent. Thymol (T) is an important component of monoterpenes and its oxidation product TQ is commercially important [30–32]. In this sense, TQ can be obtained from T using convenient catalysts (see Scheme 2). TQ is the main constituent of the volatile oil of *Nigella sativa* (black seed). Black seed belongs to the family *Ranunculaceae* and is an annual herb of the Mediterranean region, South and Central Asia, and now is also cultivated in Eastern Europe. The main active components of black seed include TQ, thymohydroquinone, dithymoquinone, thymol and carvacrol, which are important pharmacologically active substances. TQ demonstrates anticancer [33], antifungal [34], antioxidant [35–37], antinociceptive [38]

---

[*] Corresponding author. +90 322 338 60 84/2481; fax: +90 322 338 60 70.
E-mail address: bay@cu.edu.tr (B. Ay).

http://dx.doi.org/10.1016/j.poly.2014.12.043

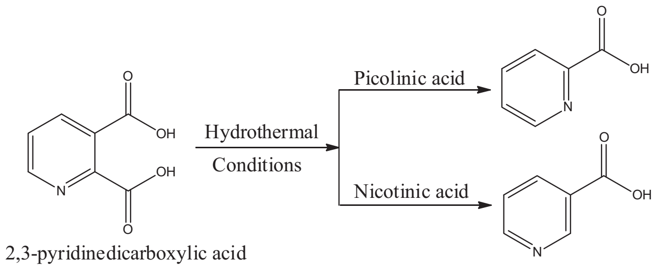

Scheme 1. The behavior of the 2,3-pydc^{2-} ligand under hydrothermal conditions.

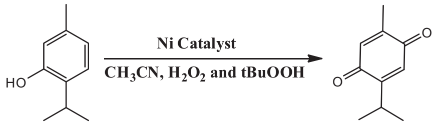

Scheme 2. Oxidation of T to TQ using a Ni(II) catalyst.

and neuropharmacological activities [39]. TQ, representing 18.4–24% of the essential oil of black seed, possesses antibacterial, antihistaminic and anti-inflammatory activities [40]. The oxidation product TQ is a crucial compound for research, such as for treatment of cancer and other diseases. Especially in the last three years, it has been proven to be effective in the treatment of cancer of the pancreas [41], breast [42,43], prostate [44] and colon [45]. Also, it has anti-microbial [46], anti-histamine [47], anti-inflammatory [48] activities and oxidative stress [49] properties.

In this article, we chose 2,3-pyridinedicarboxylic acid as a ligand because of its interesting behavior under hydrothermal conditions, and have synthesized and structurally characterized a dinuclear coordination polymer, $\{[Ni_2(NA)_4(\mu\text{-}H_2O)]\cdot 2H_2O\}_n$ (**1**). The complex was obtained with higher yield and under different conditions, such as starting materials, reaction temperature and reaction time, than complexes of similar empirical formulas [50]. The thermal property and catalytic activity of complex **1** were studied. The polymer showed high thermal stability and high selectivity in the catalytic oxidation reaction of T to TQ (Scheme 2).

2. Experimental

2.1. Materials and methods

$NiCl_2\cdot 6H_2O$, 2,3-pyridinedicarboxylic acid, NaOH, T, TQ, acetonitrile, *tert*-butyl hydroperoxide (~80%) and hydrogen peroxide (30%) were purchased from commercial sources and used as received. Hydrothermal synthesis was carried out in 23 mL PTFE-lined stainless steel containers under autogenous pressure. Infrared spectra were recorded with KBr pellets on a Perkin-Elmer RX-1 FT-IR spectrometer in the range 4000–400 cm^{-1}. Thermogravimetric analyses (TGA) were conducted in a nitrogen atmosphere with a Perkin Elmer Pyris Diamond TG/DTA equipment at a heating rate of 10 °C min^{-1}. HPLC and headspace GC/MS were used for the characterization of TQ, determination of the percentage conversion and selectivity values. The GC/MS was measured on a Thermo Brand chromatograph with TR5MS capillary columns (60 m × 0.25 mm i.d.; 25 μm film thickness). The chromatographic conditions were injector temperature: 240 °C, beginning temperature: 50 °C, final temperature: 250 °C and heating rate: 3 °C min^{-1}. For the HPLC analysis a Shimadzu HPLC system equipped with a reversed phase C8 column (250 cm × 4.6 mm column dimensions, 5 μm particle sizes, Ascentis® was used. $CH_3OH:CH_3CN:H_2O$ (50:20:30, v/v) was used for the separation as the mobile phase. The column temperature was 35 °C, the detection wavelength was 254 nm, the flow rate was 1.0 mL min^{-1} and the retention time was 15 min. Before injection of a sample, the column was equilibrated with the mobile phase at a flow-rate of 1.0 mL min^{-1} for at least 30 min or until a steady baseline was obtained. Calibration curves of T and TQ were used for determination of the conversion and yield values.

2.2. Synthesis of the coordination polymer **1**

All starting materials were used directly without further purification. A mixture of $NiCl_2\cdot 6H_2O$ (0.192 g, 0.8 mmol), pyridine 2,3-dicarboxylic acid (0.134 g, 0.8 mmol), NaOH (0.064 g, 1.6 mmol) and H_2O (5 mL, 278 mmol) in the mole ratio 1.00:1.00:2.00:348 was sealed in a 23 mL Teflon reactor and kept under autogenous pressure at 160 °C for 96 h. The mixture was cooled to room temperature at a rate of 20 °C h^{-1} and turquoise colored crystals were obtained. The heterogeneous solution mixture was separated from the solid phase and the crystals were washed with water and then dried at room temperature. Yield: 92.8% based on Ni. Initial pH: 3.60, final pH: 2.00. The coordination polymer is insoluble in common solvents (ethanol, methanol, acetonitrile etc) and water. *Anal.* Calc. for $C_{24}H_{22}N_4Ni_2O_{11}$: C, 43.64; H, 3.33; N, 8.49. Found: C, 43.12; H, 3.32; N, 8.19%. IR data (KBr pellet, cm^{-1}): 3436(w), 3103(m), 2952(m), 1605(s), 1584(s), 1491(m), 1364(s), 1006(m), 779(s), 763(s), 588(s), 516(m).

2.3. X-ray structure determination

The crystallographic data collection for **1** was performed using a Bruker AXS SMART CCD diffractometer with Mo Kα radiation at 100 K. The APEX2 Crystallographic Suite was used for determination of the unit-cell parameters. The structure was solved by direct methods and refined by full-matrix least-squares on F^2 using the SHELXTL crystallographic software package. Crystal data and structure refinement for **1** are summarized in Table 1 and selected bond lengths and angles are given in Table 2. Anisotropic displacement parameters, hydrogen coordinates and other crystallographic data are available in the Supporting Information (SI) (Tables S1–S4). A BRUKER AXS D8 model diffractometer was used for the powder X-ray diffraction of the catalyst.

2.4. Oxidation of thymol (T)

T oxidation was carried out at room temperature and at 60 °C in a three-necked flask (250 mL) equipped with a magnetic stirrer, a reflux condenser and a temperature controller in an oil bath. T (3.0 g, 20 mmol) and 20 mL acetonitrile were added successively into the flask. The appropriate amount of oxidant, 30 wt.% of aqueous H_2O_2 (7.0 mL, 69.80 mmol) and 80 wt.% aqueous of the *tert*-butyl hydroperoxide (6.0 mL, 48 mmol), were then added to the reaction mixture. After heating this mixture to 25 and 60 °C, the metal complex (0.1, 0.2 and 0.3 g) was added to start the reaction and stirred incessantly for 2, 5, 8 and 24 h. The mixture of the reactions was collected at given time intervals and was analyzed by HPLC.

3. Results and discussion

3.1. Crystal structure of $\{[Ni_2(NA)_4(\mu\text{-}H_2O)]\cdot 2H_2O\}_n$ (**1**)

The coordination polymer was synthesized hydrothermally. It is interesting to note that when the temperature was 160 °C, decarboxylation occurred and the pyridine-2,3-dicarboxylic acid was transformed into nicotinic acid in the process of the hydrothermal reaction [51,52]. Single crystal X-ray analysis showed that the

Table 1
Crystal data and structure refinement for $\{[Ni_2(NA)_4(\mu\text{-}H_2O)]\cdot 2H_2O\}_n$.

Empirical formula	$C_{24}H_{22}N_4Ni_2O_{11}$
Formula weight	659.88
T (K)	100(2)
Wavelength (Å)	0.71073
Crystal system	monoclinic
Space group	$P2(1)/c$
Unit cell dimensions	
a (Å)	10.7170(5)
b (Å)	18.7732(8)
c (Å)	13.9105(6)
α (°)	90
β (°)	103.0500(10)
γ (°)	90
V (Å^3)	2726.4(2)
Z	4
D_{calc} (g cm^{-3})	1.608
Absorption coefficient (mm^{-1})	1.447
$F(000)$	1352
Crystal size (mm)	0.30 × 0.24 × 0.20
Theta range for data collection (°)	1.85–25.35
Index ranges	$-12 \leqslant h \leqslant 12$, $-22 \leqslant k \leqslant 22$, $-16 \leqslant l \leqslant 16$
Reflections collected	22926
Independent reflections (R_{int})	4989 (0.0559)
Completeness to theta = 25.00°	99.9%
Absorption correction	multi-scan
Refinement method	Full-matrix least-squares on F^2
Data/restraints/parameters	4989/6/388
Goodness-of-fit (GOF) on F^2	1.146
Final R indices [$I > 2\sigma(I)$]	$R_1 = 0.0358$, $wR_2 = 0.0871$
R indices (all data)	$R_1 = 0.0436$, $wR_2 = 0.0894$
Largest difference in peak and hole (e Å^{-3})	0.454 and −0.511

Table 2
Selected bond lengths [Å] and angles [°] for $\{[Ni_2(NA)_4(\mu\text{-}H_2O)]\cdot 2H_2O\}_n$.

Ni(1)–O(8)	2.0022(19)	Ni(2)–N(4)#4	2.103(2)
Ni(1)–O(4)#1	2.0579(19)	Ni(2)–N(2)	2.110(2)
Ni(2)–O(7)	2.116(2)	Ni(1)–N(1)#2	2.070(3)
Ni(2)–O(9)	2.118(2)	Ni(1)–N(3)	2.084(2)
Ni(1)–O(1)	2.100(2)	O(6)–Ni(2)#5	2.050(2)
Ni(1)–O(9)	2.123(2)	N(1)–Ni(1)#2	2.070(3)
Ni(2)–O(2)	2.033(2)	N(4)–Ni(2)#4	2.103(2)
O(8)–Ni(1)–O(4)#1	174.25(8)	N(1)#2–Ni(1)–O(1)	87.18(9)
O(8)–Ni(1)–N(1)#2	90.87(9)	N(3)–Ni(1)–O(1)	177.42(9)
O(4)#1–Ni(1)–N(1)#2	88.00(9)	O(8)–Ni(1)–O(9)	92.18(8)
O(8)–Ni(1)–N(3)	90.32(9)	O(4)#1–Ni(1)–O(9)	88.96(8)
O(4)#1–Ni(1)–N(3)	95.33(9)	N(1)#2–Ni(1)–O(9)	176.95(8)
N(1)#2–Ni(1)–N(3)	90.61(10)	O(6)#3–Ni(2)–O(7)	82.35(8)
O(8)–Ni(1)–O(1)	91.05(8)	N(4)#4–Ni(2)–O(7)	91.11(9)

Symmetry transformations used to generate equivalent atoms: #1 −x, −y, −z + 1 #2 −x + 1, −y, −z + 1 #3 x, −y + 1/2, z + 1/2 #4 −x + 1, −y, −z + 2 #5 x, −y + 1/2, z−1/2.

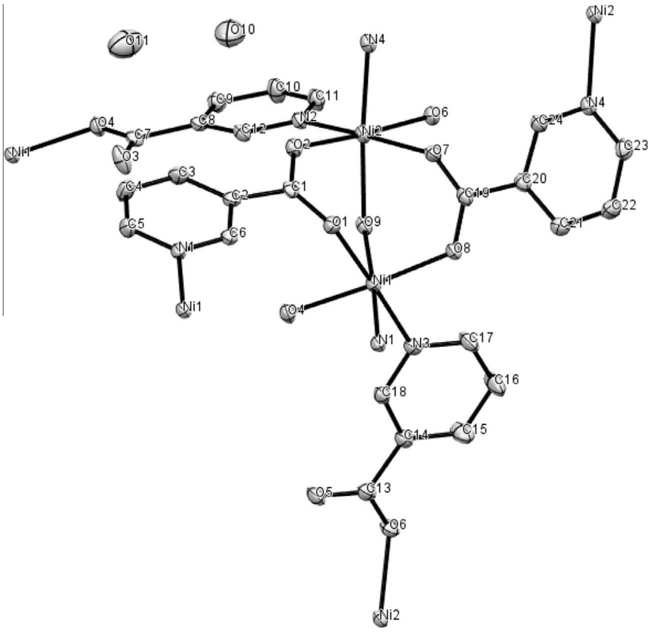

Fig. 1. ORTEP view of the coordination environment of the Ni(II) ion in compound **1**. Thermal ellipsoids are drawn at the 30% probability level. All hydrogen atoms have been omitted for clarity.

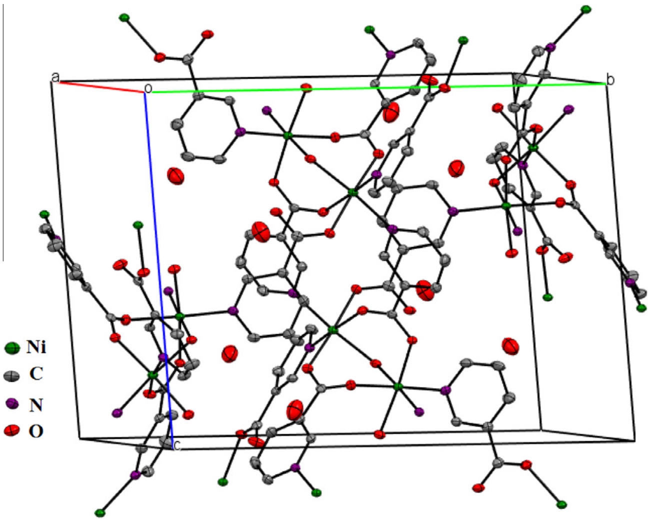

Fig. 2. The three-dimensional network of **1** (hydrogen atoms have been removed for clarity).

structure of compound **1** exhibits an interesting infinite three-dimensional (3D) network, in which the symmetric, neutral and dimeric complex unit contains two Ni atoms, four NA anions and a bridge water molecule (Fig. 1), unlike that of Ref. [50]. There are two independent Ni ions and the bridging carboxylates form a double-sided structure. Each nickel ion in the complex is six-coordinate, with an approximate octahedral geometry where the equatorial plane is made up of one N and three O donors from four independent NA anions. The axial sites are occupied by one N donor from one NA anion and one O atom from the water molecule. Each asymmetrical unit is linked via Ni-O–Ni bridges and H-bonds. The nickel(II) ions in the coordination polymer are bridged by bidentate nicotinic acid groups (μ-η^1-carboxylate) (Fig. 2). The structure of 1 also involves two non-coordinated water molecules in each unit cell. The Ni–N bond distances range from 2.050(2) to 2.110(2) Å, while those of Ni–O are from 2.0022(19) to 2.123(2) Å; the O–Ni–O bond angles range from 82.35(8)° to 174.25(8)° and those of O–Ni–N are from 88.00(9)° to 95.33(9)°, which is consistent with values reported for other nickel(II)-carboxylates [53,54] (see Table 2).

3.2. IR spectra

In the FT-infrared spectrum, the ligand 2,3-pydc^{2-} shows stretching bands attributed to ν(O-H), ν(C=O), ν(C=N) and ν(C–H) at 3409, 1632, 1583 and 1112 cm^{-1}, respectively (SI, Fig. S1). The FT-IR spectrum of the coordination polymer displays a broad absorption band at about 3436 cm^{-1} for the stretching vibrations of ν(O–H) groups [55,56] engaged in hydrogen bonds (non-coordinated and bridge H_2O molecules). The strong vibrations appearing at 1605 and 1584 cm^{-1} correspond to asymmetric and symmetric

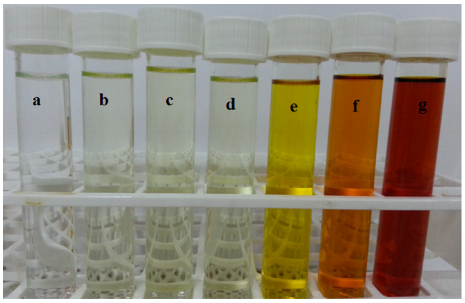

Scheme 3. Oxidation production of T using H_2O_2 as an oxidant at room temperature and 60 °C. (a) Without catalyst; (b) 25 °C – 0.1 g catalyst; (c) 25 °C – 0.2 g catalyst; (d) 25 °C – 0.3 g catalyst; (e) 60 °C – 0.1 g catalyst; (f) 60 °C – 0.2 g catalyst; (g) 60 °C – 0.3 g catalyst.

stretching vibrations of the carboxylate groups [57], indicating the carboxylate oxygen atoms are coordinated to the metal center. Broad absorption bands at about 3103, 2952 and 1491 cm^{-1} can be assigned to the aromatic and aliphatic stretching vibrations of ν(C–H) and ν(C=N) bonds of the pyridine rings [58], respectively. The remarkable changes observed in the 800–400 cm^{-1} region for the complex are attributed to the coordination of the ligands to the metal. New bands of very strong intensities at 588 and 516 cm^{-1} can be assigned to the ν(Ni–N) [59] and ν(Ni–O) [60] modes, respectively (SI, Fig. S2).

3.3. Thermal stability

TG analysis was used to examine the thermal stability of the coordination polymer, (SI, Fig. S3). It was performed in the temperature range of 25–800 °C under a N_2 atmosphere at 1 atm, with a heating rate of 10 °C min^{-1} on a Perkin Elmer Diamond TG/DTA. The compound is thermally stable up to 158 °C. The TGA curve exhibits three steps of weight losses above this temperature. The first weight loss of 22.33% between 158 and 206 °C is attributable to the loss of non-coordinating and one organic ligand in the formula unit (calculated: 23.94%). The second significant weight loss of 35.16% between 350 and 411 °C, corresponds to the decomposition of two organic ligands (calculated: 36.98%). The third weight loss of 19.60% between 460 and 660 °C, corresponds to the decomposition of the remaining ligand (calc. 18.48%). The remaining weight of 22.91% corresponds to the percentage of metal (20.60%) and oxide components, indicating that the final product is NiO. The thermal results fundamentally agree with the structure of 1 and the observed thermal behavior reflects the structural features.

3.4. Catalytic activity

An important disadvantage of homogeneous catalysts is the difficulty of their recovery from the reaction medium and their poor thermal stability. In comparison, heterogeneous catalysts usually have better thermal stability and the catalyst can be easily retrieved from the reaction medium by filtration. TBHP has seldom been used as an oxidant in investigations on the catalytic efficiency of nickel(II) complexes towards oxidation reactions in a heterogeneous medium. Hydrogen peroxide and *tert*-butyl hydroperoxide (TBHP) are inexpensive and environmental friendly oxidant reagents. To the best of our knowledge, *tert*-butyl hydroperoxide has not been previously used for the oxidative conversion of T to TQ [61]. It should also be noted that there was no oxidation product TQ (trace amounts) using only H_2O_2 or TBHP as an oxidant without a catalyst (see Scheme 3a). This result was supported by HPLC analysis (SI, Fig. S4). When using the catalyst, T was oxidized to TQ (see Scheme 3b–g). On the other hand, when the oxidation reaction was carried out with solely the Ni(II) salt, TQ was only obtained in trace amounts. Headspace GC/MS analysis was used for the characterization of the oxidation product TQ (SI, Fig. S5). The performance of the catalyst was determined using HPLC. Acetonitrile as a solvent, hydrogen peroxide and *tert*-butyl hydroperoxide as oxidants were used in the catalytic reactions. T conversion values under different reaction conditions are given in Table 3. The calibration curves of the compounds were used for calculation of the conversion values (SI, Fig. S6). Before the catalytic reactions, the retention times of T and TQ were determined by chromatographic analysis (SI, Fig. S7). As a result of GC/MS and HPLC analyses, no product other than the main product TQ was observed at the end of the catalytic studies using both hydrogen peroxide and *tert*-butyl hydroperoxide (SI, Figs. S8 and S9).

Table 3
Conversion of T with acetonitrile as the solvent under different reaction conditions (catalyst: $\{[Ni_2(NA)_4(\mu\text{-}H_2O)]\cdot 2H_2O\}_n$).

H_2O_2				*tert*-Butyl hydroperoxide			
Temperature (°C)	Catalyst amount (g)	Reaction time (h)	Thymol conversion (%)	Temperature (°C)	Catalyst amount (g)	Reaction time (h)	(%)
25	0.1	2	0.23	25	0.1	2	0.10
		5	0.53			5	0.13
		8	3.26			8	0.24
		24	4.74			24	0.40
	0.2	2	0.64		0.2	2	0.22
		5	2.05			5	0.27
		8	4.55			8	0.51
		24	5.95			24	1.34
	0.3	2	2.50		0.3	2	2.34
		5	4.51			5	3.11
		8	6.22			8	3.70
		24	7.94			24	4.20
60	0.1	2	3.44	60	0.1	2	5.65
		5	4.64			5	7.74
		8	8.21			8	8.22
		24	10.70			24	9.38
	0.2	2	5.69		0.2	2	4.22
		5	9.80			5	6.43
		8	13.32			8	10.40
		24	21.15			24	12.44
	0.3	2	10.66		0.3	2	6.20
		5	13.72			5	8.60
		8	23.23			8	12.87
		24	31.08			24	18.28

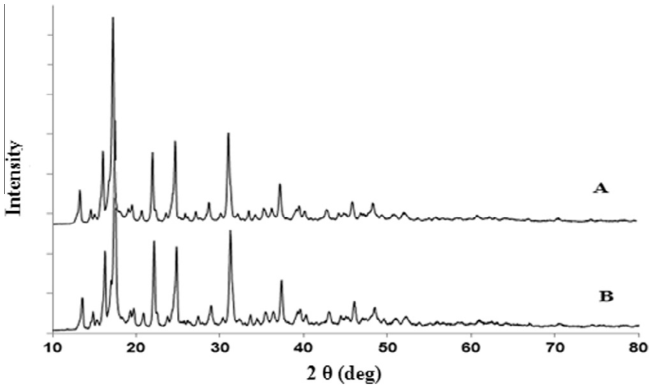

Fig. 3. XRD patterns for **1** (A) before the catalaytic reaction; (B) after using **1** as a catalyst four times for 24 h at 60 °C.

To determine the activity of the catalyst, the T conversion was plotted at room temperature and 60 °C. The other variables were 0.1, 0.2 and 0.3 g catalyst amounts, hydrogen peroxide and *tert*-butyl hydroperoxide as oxidants and different reaction times. Although the conversion values were 18.28% with TBHP, 31.08% with H_2O_2, their selectivities were approximately 100%. HPLC analyses were carried out after different reaction times (2, 5, 8 and 24 h) to determinate the performance of the catalyst (SI, Figs. S8 and S9). The catalyst activity was optimized with 0.3 g (0.45 mmol) of complex and using H_2O_2 as an oxidant. The maximum T conversion was 31.08% after 24 h with approximately 100% selectivity at 60 °C. The catalytic performance of the nicotinic acid was measured under the same catalytic conditions. First of all, the oxidation reaction was performed without catalyst and trace amounts of thymoquinone were observed (SI, Fig. S4). Afterwards, nicotinic acid was used as a catalyst under the same conditions. The HPLC studies (SI, Fig. S10) showed that trace amounts of thymoquinone were observed using nicotinic acid. These studies support that nicotinic acid does not show any catalytic activity for the oxidation of thymol to thymoquinone, with results analogous to those without catalyst.

3.5. Separation and reusability of the catalyst

Easy separation of the catalyst from the reaction medium is the most important advantage of heterogeneous catalysts. Determination of the phase purity and recycling experiments for the sample were proven with XRD and elemental analysis (SI, Table S5) techniques. Four sequentially reactions was performed for 0.3 g (0.45 mmol) catalyst, using hydrogen peroxide and 24 h with a 60 °C reaction temperature. To determine the reusability of the catalyst, it was separated from the reaction mixture, filtered off, washed with ethanol (10 mL), water (50 mL) and acetone (10 mL), then dried in a vacuum oven at 45 °C and reused. No traces of the metal in the filtrate were observed. The conversion values did not decrease significantly after four tests (SI, Table S6). These results show that the catalyst has long usability in the oxidation reaction. Powder XRD analysis was carried out to determine the crystallinity of the catalyst before and after using it in the reaction. The results of the XRD analysis showed no differences in the patterns of the catalyst (Fig. 3). This means that the crystallinity of the catalyst was unchanged (the crystallinity data are given in the SI, Table S7). Also, the presence of nickel ions in the solution was checked by ICP-MS analysis. The results showed that there were no nickel ions in the solution.

4. Conclusion

A dinuclear nickel(II) coordination polymer, based on the dimer $[Ni_2(NA)_4(\mu\text{-}H_2O)]\cdot 2H_2O$, has been synthesized from a solution of $NiCl_2\cdot 4H_2O$, 2,3-pydcH_2, NaOH and H_2O by the hydrothermal method and it has been characterized structurally. We used 2,3-pydcH_2 as a different starting ligand from that of Ref. [50], but it is interesting that it turned into nicotinic acid under the hydrothermal conditions, giving an interesting 3D network structure. Also their geometric structures were different from each other [50]. The synthesized polymer showed high selectivity (100%) and good conversions (31.08%) in the oxidation of T. This percent conversion is higher than the values of 20 and 18% from related catalytic studies [62,63]. The results from our previous [30,64] and current studies revealed that catalysts synthesized under hydrothermal conditions can show high selectivity because of their high purities and crystallinity. Our research is moving towards the synthesis of effective catalysts having higher conversions of TQ from T, TQ being a precious and expensive compound. In the next step, pure TQ will be separated from T.

Acknowledgement

The authors gratefully acknowledge financial support from the Research Unit of Çukurova University (Grant No. FEF2013D5).

Appendix A. Supplementary data

CCDC 1004678 contain the supplementary crystallographic data for complexes **1**, respectively. These data can be obtained free of charge via http://www.ccdc.cam.ac.uk/conts/retrieving.html, or from the Cambridge Crystallographic Data Centre, 12 Union Road, Cambridge CB2 1EZ, UK; fax: (+44) 1223-336-033; or e-mail: deposit@ccdc.cam.ac.uk. Supplementary data associated with this article can be found, in the online version, at http://dx.doi.org/10.1016/j.poly.2014.12.043.

References

[1] (a) B. Moulton, M.J. Zaworotko, Chem. Rev. 101 (2001) 1629;
(b) K.T. Holman, A.M. Pivovar, J.A. Swift, M.D. Ward, Acc. Chem. Rev. 34 (2001) 107;
(c) S.H. Feng, R.R. Xu, Acc. Chem. Res. 34 (2001) 239;
(d) L. Carlucci, G. Ciani, D.M. Proserpio, Coord. Chem. Rev. 246 (2003) 247;
(e) M. Fujita, Y.J. Kwon, S. Washizu, K. Ogura, J. Am. Chem. Soc. 116 (1994) 1151.
[2] T.M. Smith, A. Lau, J. Zubieta, Inorg. Chim. Acta 409 (2014) 296.
[3] T.M. Smith, L. Strauskulage, K.A. Perrin, J. Zubieta, Inorg. Chim. Acta 407 (2013) 48.
[4] (a) J.H. He, J.H. Yu, Y.T. Zhang, Q.H. Pan, R.R. Xu, Inorg. Chem. 44 (2005) 9279;
(b) H. Yin, S.X. Liu, Polyhedron 26 (2007) 3103;
(c) Y.H. Zhao, Z.M. Su, Y.M. Fu, K.Z. Shao, P. Li, Y. Wang, X.R. Hao, D.X. Zhu, S.D. Liu, Polyhedron 27 (2008) 583;
(d) C.D. Ene, F. Tuna, O. Fabelo, C. Ruiz-Perez, A.M. Madalan, H.W. Roesky, M. Andruh, Polyhedron 27 (2008) 574.
[5] (a) S.-I. Noro, S. Kitagawa, M. Yamashita, T. Wada, Chem. Commun. (2002) 222;
(b) SM. Humphrey, P.T. Wood, J. Am. Chem. Soc. 126 (2004) 13236;
(c) X.L. Wang, C. Qin, E.B. Wang, Y.G. Li, N. Hao, C.W. Hu, L. Xu, Inorg. Chem. 43 (2004) 1850;
(d) M.L. Tong, J. Wang, S. Hu, S.R. Batten, Inorg. Chem. Commun. 8 (2005) 48.
[6] H. Yin, S.-X. Liu, J. Mol. Struct. 918 (2009) 165.
[7] B. Zhao, P. Cheng, Y. Dai, C. Cheng, D.Z. Liao, S.P. Yan, Z.H. Jiang, J.L. Wang, Angew. Chem., Int. Ed. Engl. 42 (2003) 934.
[8] M.L. Tong, J. Wang, S. Hu, J. Solid State Chem. 178 (2005) 1518.
[9] B. Zhao, H.L. Guo, X.L. Cheng, P. Cheng, W. Shi, D.Z. Liao, S.P. Yan, Z.H. Jiang, Chem. Eur. J. 12 (2006) 149.
[10] H.L. Guo, B. Ding, L. Yi, P. Cheng, D.Z. Liao, S.P. Yan, Z.H. Jiang, Inorg. Chem. Commun. 8 (2005) 151.
[11] J.C. MacDonald, T.J.M. Luo, G.T.R. Palmore, Cryst. Growth Des. 4 (2004) 1203.
[12] S.X. Cui, Y.L. Zhao, J.P. Zhang, Q. Liu, Y. Zhang, Cryst. Growth Des. 8 (2008) 3803.
[13] M.S. Liu, Q.Y. Yu, Y.P. Cai, C.Y. Su, X.M. Lin, X.X. Zhou, J.W. Cai, Cryst. Growth Des. 8 (2008) 4083.
[14] L.L. Wen, Y.Z. Li, Z.D. Lu, J.G. Lin, C.Y. Duan, Q.J. Meng, Cryst. Growth Des. 6 (2006) 530.
[15] B.O. Patrick, C.L. Stevens, A. Storr, R.C. Thompson, Polyhedron 22 (2003) 3025.
[16] A.M. Beatty, B.A. Helfrich, G.A. Hogan, B.A. Reed, Cryst. Growth Des. 6 (2006) 122.

[17] J.C. MacDonald, P.C. Dorrestein, M.M. Pilley, M.M. Foote, J.L. Lundburg, R.W. Henning, A.J. Schultz, J.L. Manson, J. Am. Chem. Soc. 122 (2000) 11692.
[18] S.K. Ghosh, J. Ribas, P.K. Bharadwaj, CrystEngComm 6 (2004) 250.
[19] N.H. Hu, Z.G. Li, J.W. Xu, H.Q. Jia, J.J. Niu, Cryst. Growth Des. 7 (2007) 15.
[20] D. Deng, P. Liu, W. Fu, L. Li, F. Yang, B. Ji, Inorg. Chim. Acta 363 (2010) 891.
[21] Q. Yue, J. Yang, G.-H. Li, G.-D. Li, W. Xu, J.-S. Chen, S.-N. Wang, Inorg. Chem. 44 (2005) 5241.
[22] M. Li, J.-F. Xiang, L.-J. Yuan, S.-M. Wu, S.-P. Chen, J.-T. Sun, Cryst. Growth Des. 6 (2006) 2036.
[23] P. Sengupta, S. Ghosh, T.C.W. Mark, Polyhedron 20 (2001) 975.
[24] L.A. Gerrard, P.T. Wood, Chem. Commun. (2000) 2107
[25] L. Chen, X.-M. Lin, Y. Ying, Q.-G. Zhan, Z.-H. Hong, J.-Y. Li, N.S. Weng, Y.-P. Cai, Inorg. Chem. Commun. 12 (2009) 761.
[26] Z.B. Han, X.N. Cheng, X.M. Chen, Cryst. Growth Des. 5 (2005) 695.
[27] Z.B. Han, X.N. Cheng, X.F. Li, X.M. Chen, Z. Anorg. Allg. Chem. 631 (2005) 642.
[28] Z.-B. Han, Y. Ma, Z.-G. Sun, W.-S.g. You, Inorg. Chem. Commun. 9 (2006) 844.
[29] T. Whitfield, L.-M. Zheng, X. Wang, A.J. Jacobson, Solid State Sci. 3 (2001) 829.
[30] B. Ay, E. Yildiz, S. Jones, J. Zubieta, Inorg. Chim. Acta 387 (2012) 15.
[31] R.S. Dowining, H. van Bekkum, R.A. Sheldon, Cattech 95, December 1997.
[32] Sopharma USA Coorporation, 2001. <http://www.sopharma.com/categories/447/44704 rhinolex.html>.
[33] M.L. Salem, Int. Immunopharmacol. 5 (2005) 1749.
[34] S. Hamad, M. Aljabre, M.A. Randhawa, N. Akhtar, O.M. Alakloby, A.M. Alqurashi, A. Aldossary, J. Ethnopharmacol. 101 (2005) 116.
[35] M. Ismail, G. Al-Naqeep, K.W. Chan, Free Radical Biol. Med. 48 (2010) 664.
[36] H.S. El-Abhar, D.M. Abdallah, S. Saleh, J. Ethnopharmacol. 84 (2003) 251.
[37] H. Lutterodt, M. Luther, M. Slavin, J. Yin, J. Parry, J. Gao, L.L. Yu, LWT-Food Sci. Technol. 43 (2010) 1409.
[38] A.-F.M. Abdel-Fattah, K. Matsumoto, H. Watanabe, Eur. J. Pharmacol. 400 (2000) 89.
[39] T.B. Al-Naggar, M.P. Gómez-Serranillos, M.E. Carretero, A.M. Villar, J. Ethnopharmacol. 88 (2003) 63.
[40] M. Toghyani, M. Toghyani, A. Gheisari, G. Ghalamkari, M. Mohammadrezaei, Livest. Sci. 129 (2010) 173.
[41] M. Yusufi, S. Banerjee, M. Mohammad, S. Khatal, K.V. Swamy, E.M. Khan, A. Aboukameel, F.H. Sarkar, S. Padhye, Bioorg. Med. Chem. Lett. 23 (2013) 3101.
[42] S. Rajput, B.N.P. Kumar, K.K. Dey, I. Pal, A. Parekh, M. Mandal, Life Sci. 93 (2013) 783.
[43] K.M. Sutton, C.D. Doucette, D.W. Hoskin, Biochem. Biophys. Res. Commun. 426 (2012) 421.
[44] C.C. Woo, A.P. Kumar, G. Sethi, K.H.B. Tan, Biochem. Pharmacol. 83 (2012) 443.
[45] H. Jrah-Harzallaha, S. Ben-Hadj-Khalifa, A. Maloul, R. El-Ghali, T. Mahjoub, J. Funct. Foods 5 (2013) 1310.
[46] H.J. Harzallah, B. Kouidhi, G. Flamini, A. Bakhrouf, T. Mahjoub, Food Chem. 129 (2011) 1469.
[47] M. Toghyani, M. Toghyani, A. Gheisari, G. Ghalamkari, M. Mohammadrezaei, Livest. Sci. 129 (2010) 173.
[48] C.C. Woo, A.P. Kumar, G. Sethi, K.H.B. Tan, Biochem. Pharmacol. 83 (2012) 443.
[49] M.N. Nagi, H.A. Almakki, M.M. Sayed-Ahmed, A.M. Al-Bekairi, Food Chem. Toxicol. 48 (2010) 2361.
[50] A.E. Wasson, R.L. LaDuca, Polyhedron 26 (2007) 1001.
[51] W. Chen, H.-M. Yuan, J.-Y. Wang, Z.-Y. Liu, J.-J. Xu, M. Yang, J.-S. Chen, J. Am. Chem. Soc. 125 (2003) 9266.
[52] M. Li, J. Xiang, L. Yuan, S. Wu, S. Chen, J. Sun, Cryst. Growth Des. 6 (9) (2006).
[53] D.-X. Hu, P.-K. Chen, F. Luo, L. Xue, Y. Che, J.-M. Zheng, Inorg. Chim. Acta 360 (2007) 4077.
[54] Y.-G. Huang, Y.-F. Zhou, D.-Q. Yuan, B.-L. Wu, F.-L. Jiang, M.-C. Hong, J. Mol. Struct. 830 (2007) 85.
[55] M.M. Najafpour, V. McKee, Catal. Commun. 11 (2010) 1032.
[56] M. Cai, J. Chen, M. Taha, Inorg. Chem. Commun. 13 (2010) 199.
[57] R. Łyszczek, J. Anal. Appl. Pyrol. 86 (2009) 239.
[58] E. Soleimani, J. Mol. Struct. 995 (2011) 1.
[59] J.M. Ramosa, O. Versiane, J. Felcman, C.A.T. Soto, Spectrochim. Acta, Part A 67 (2007) 1037.
[60] B. Macíasa, M.V. Villaa, I. Rubioa, A. Castiñeirasb, J. Borra, J. Inorg. Biochem. 84 (2001) 163.
[61] H. Wojtowicz, M. Brzaszcz, K. Kloc, J. Mlochowski, Tetrahedron 57 (2001) 9743.
[62] F.C. Skrobot, A. Valente, G. Neves, I. Rosa, J. Rocha, J.A.S. Cavaleiro, J. Mol. Catal. A 201 (2003) 211.
[63] I.C.M.S. Santos, M.M.Q. Simões, M.M.M.S. Pereira, R.R.L. Martins, M.G.P.M.S. Neves, J.A.S. Cavaleiro, A.M.V.J. Cavaleiro, Mol. Catal. A 195 (2003) 253.
[64] B. Ay, E. Yildiz, J.D. Protasiewicz, A.L. Rheingold, Inorg. Chim. Acta 399 (2013) 208.